Effects of core stochastization on particle and momentum transport

doi: 10.1088/1741-4326/abd6b1

LETTER • OPEN ACCESS

Effects of core stochastization on particle and momentum transport

OPEN ACCESS
IOP Publishing | International Atomic Energy Agency Nuclear Fusion
Nucl. Fusion **61** (2021) 034002 (6pp) https://doi.org/10.1088/1741-4326/abd6b1

Letter

Effects of core stochastization on particle and momentum transport

Yoshiaki Ohtani[1,*], Kenji Tanaka[2], Hiroe Igami[2], Katsumi Ida[2], Yasuhiro Suzuki[2], Yuki Takemura[2], Hayato Tsuchiya[2], Mike Sanders[3], Mikirou Yoshinuma[2], Tokihiko Tokuzawa[2], Ichihiro Yamada[2], Ryo Yasuhara[2], Hisamichi Funaba[2], Mamoru Shoji[2], Takahiro Bando[1] and LHD Experimental Group[2]

[1] Naka Fusion Institute, National Institutes for Quantum and Radiological Science and Technology, 801-1 Mukoyama, Naka, Ibaraki, 311-0193, Japan
[2] National Institute for Fusion Science, 322-6 Oroshi, Toki, Gifu 509-5292, Japan
[3] Eindhoven University of Technology, Eindhoven, 5600 MB, Netherlands

E-mail: ohtani.yoshiaki@qst.go.jp

Received 29 September 2020, revised 27 November 2020
Accepted for publication 24 December 2020
Published 12 February 2021

Abstract

The effects of the stochastic magnetic field in a plasma center produced by electron cyclotron current drive (ECCD) on transport have been revealed. Because the electron temperature profile is flat in the core region, in the case of counter-directed ECCD (ctr-ECCD) against the toroidal magnetic field, the magnetic field is stochastic in the core region with rotational transform $\iota \sim 1/3$. The particle diffusion coefficient of the ctr-ECCD plasma is approximately 20 times as large as that of the plasma without the stochastic magnetic field produced by co-directed ECCD (co-ECCD) at the maximum. Furthermore, in the stochastic magnetic field with ctr-ECCD, counter-directed intrinsic rotation is observed in the plasma with balanced NBI discharge.

Keywords: stochastic magnetic field, particle transport, momentum transport, helical device, modulation experiment

(Some figures may appear in colour only in the online journal)

1. Introduction

The stochastic magnetic field affects transport properties and can be used as one of the techniques to control plasmas. Thus, understanding the effects of the stochastic magnetic field on particle, thermal, and momentum transport is one of the important issues for fusion plasmas. For example, the stochastic magnetic field produced by the external perturbation field at the plasma edge induces co-current-directed torque and enhances transport in the tokamak plasma [1, 2]. Experimentally, the edge stochastization produced by an edge-resonant magnetic perturbation can suppress impulsive bursts of edge-localized modes in high-confinement mode (H-mode) without changing the H-mode transport barrier and core confinement [3]. On the other hand, the core stochastization degrades the confinement of plasmas in the core. In reversed field pinch devices, transport under stochastization is investigated from a power balance analysis [4], and suppression of the core stochastization by controlling the current density profile improves confinement [5].

* Author to whom any correspondence should be addressed.

Core stochastization is observed and its effects on transport have been studied in the large helical device (LHD). In LHD, the magnetic topologies of a nested magnetic flux surface, magnetic islands, and the stochastic magnetic field can be controlled by using external coils and plasma current by neutral beam injection (NBI) [6–9]. In a previous work in LHD, the core stochastic magnetic field was found to enhance electron thermal transport [8]. Ion thermal transport is less affected by the core stochastic magnetic field because the thermal velocity of the ions is lower than that of the electrons [8]. The stochastization also affects the toroidal flow via the damping (increase of effective viscosity) and driving by the non-diffusive term. Although the response of heat transport and momentum transport in the stochastic plasma were observed, the profile shape of the density was not significantly different before and after the stochastization. Then, particle transport was not evaluated due to the constant particle fueling in time, thus the effects of the stochastic magnetic field on particle transport are not fully understood [8].

In this letter, we show the experimental results of plasmas with/without the local core stochastic magnetic field produced by changing the direction of the localized core plasma current using electron cyclotron resonant heating (ECRH) [10, 11]. Using a density modulation experiment, particle transport is compared between stochastic/non-stochastic plasmas. Furthermore, the difference in the toroidal rotation is also observed. From these results, the effects of stochastization on particle and momentum transport are discussed.

2. Experimental condition and results

A density modulation experiment has been performed in hydrogen plasma under the following conditions. The magnetic configuration is the so-called inward-shifted configuration [12], which is $R_{ax} = 3.6$ m and $\mathbf{B}_{ax} = 2.75$ T, where R_{ax} and $\mathbf{B}_{ax}$ are the position of the magnetic axis and a toroidal magnetic field at R_{ax}, respectively. The plasmas are heated by 3.7 MW of negative ion-based NBI (N-NBI) and 2.8 MW of ECRH with 77 GHz and 154 GHz, which are injected in a tangential direction, from 3.3–5.3 s. The injection direction of ECRH in the LHD can be controlled. The direction of the ECCD can be controlled by the injection direction of the ECRH [13]. The core localized plasma current due to ECCD changes the poloidal magnetic field. Thus, the magnetic topology is controlled by the injection direction of ECRH. The N-NB is injected in order to measure the magnetic shear $(= (\rho/\iota)(\partial\iota/\partial\rho))$ by motional Stark effect (MSE) spectroscopy [14]. The two N-NBs are injected in the co- and ctr-direction, then the external tangential torque can be canceled out with them, amounting to a few percent of the driving force from each tangential NB [15]. In addition, the ECRH does not contribute to the torque input. Thus, the observed toroidal rotation is the intrinsic rotation. The ECRH is injected in the counter direction for #151913 (ctr-ECCD plasma), the co-direction for #151919 (co-ECCD plasma), and a balanced injection for #151916 (bal-ECCD plasma). The plasma current in the core region can be controlled by the injection direction of ECRH. As a result, the rotational transform, magnetic shear, and rational surface can be controlled [13, 16].

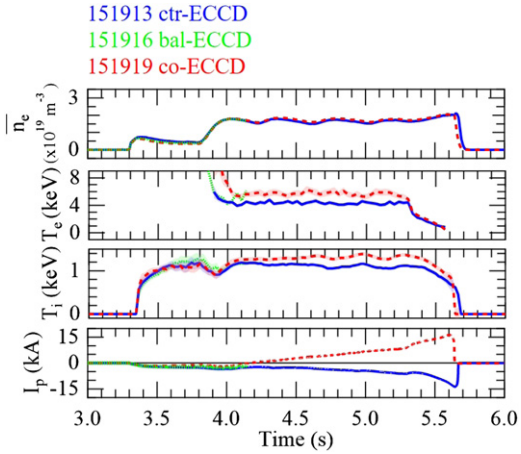

Figure 1. Temporal waveform of (*a*) line-averaged density, (*b*) T_e at $\rho = 0$, (*c*) central ion temperature from Ar^{+17}, and (*d*) plasma current. A positive sign of I_p indicates co-directed I_p. Blue solid lines and red dashed lines indicate the ctr-ECCD plasma and the co-ECCD plasma, respectively.

Figure 1 shows the temporal waveforms of #151913, #151916, and #151919. Note that the temporal waveforms of #151916 are shown until $t = 4.15$ s because the NB was broken down in the bal-ECCD plasma discharge at $t = 4.15$ s. The line-averaged density $\bar{n}_e$ is modulated between 1.6–1.8 $\times$ 10^{19} m^{-3} by conventional gas puffing with a modulation frequency of 2.5 Hz during an analysis time window of 4.0–5.2 s. The electron temperature T_e obtained with Thomson scattering measurement and the ion temperature T_i in the plasma center obtained with Ar^{+17} of the ctr-ECCD plasma are 20%–30% and 5%–20% lower than those of the co-ECCD plasma, respectively. Due to the ECRH, the direction of the plasma current I_p of the ctr-ECCD plasma is opposite to that of the co-ECCD plasma. This observation indicates that the plasma current direction is not determined by the bootstrap current but by the ECCD, because the edge pressure gradient is similar in both cases.

Figure 2 shows the rotational transform ι obtained with MSE at $t = 4.6$ s, the profiles of n_e, T_e, T_i averaged in the analysis time window, and V_{tor} profiles at $t = 4.6$ s for the co- and the ctr-ECCD plasmas. In the bal-ECCD case, the profiles of ι, V_{tor}, and T_i at $t = 4.0$ s and the profiles of n_e, T_e averaged at $t = 4.0$–4.1 s are shown in figure 2. Here, ρ is defined as a normalized effective minor radius by a_{99}, which indicates the effective minor radius inside which 99% of the electron kinetic energy exists [17]. The localized current in the plasma core can be produced by ECCD and the current can change the rotational transform. As shown in figure 2(*a*), ι reaches 1/3 at $\rho \sim 0.3$ in the ctr-ECCD case, ι reaches 1/3 at $\rho \sim 0.2$ in the bal-ECCD case, and ι reaches 1/2 in the co-ECCD case. In the case of the ctr-ECCD plasma, the T_e profile is flat at $\rho < 0.3$ where ι reaches 1/3, as shown in figure 2(*c*). This indicates the existence of large electron thermal diffusion in the ctr-ECCD plasma. This T_e flattening strongly suggests the existence of a stochastic magnetic field at $\rho < 0.3$. In the

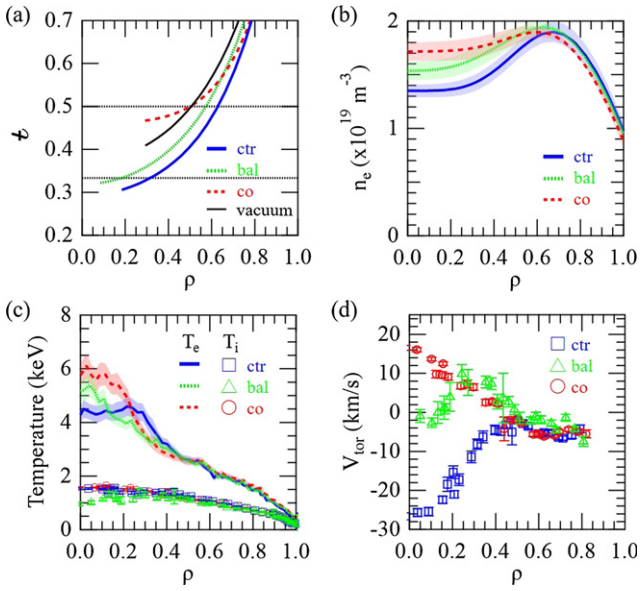

Figure 2. (*a*) ι profiles. A black solid line indicates the ι profile in the vacuum, and black dashed lines indicate the rational surface of $\iota = 1/3$ and $1/2$. (*b*) The n_e profiles. (*c*) The T_e profiles and the T_i profiles. (*d*) The V_{tor} profiles. The blue, green, and red plots and lines indicate the ctr-, the bal-, and the co-ECCD data, respectively. In (*a*) and (*d*), the data of the ctr- and the co-ECCD plasmas at $t = 4.6$ s, and the data of the bal-ECCD plasma at $t = 4.0$ s are shown. In (*b*) and (*c*), the averaged value of the ctr- and the co-ECCD plasmas at $t = 4.0$–5.2 s, and the averaged value of the bal-ECCD plasma at $t = 4.0$–4.1 s are shown.

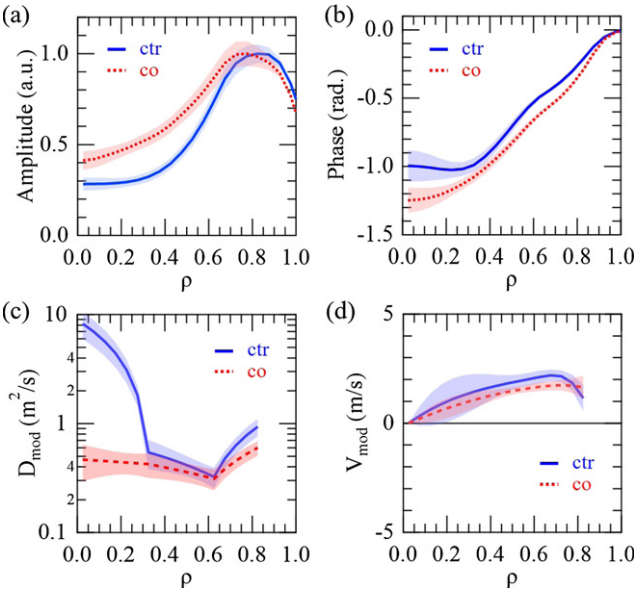

Figure 3. (*a*) Amplitude and (*b*) phase profiles of the modulation. (*c*) D_{mod} and (*d*) V_{mod} profiles. Blue solid lines and red dot lines indicate the ctr- and the co-ECCD plasma, respectively.

bal-ECCD case, although ι reaches 1/3, the T_e profile is not flat. Thus, stochastization should not occur in the bal-ECCD case. It should be noted that MHD modes are not observed in the core. The n_e profiles shown in figure 2(*b*) are reconstructed from the line-integrated density n_eL obtained with a 13 ch FIR laser interferometer [18, 19] by using Tikhonov Phillips regularization and generalized cross-validation [20, 21]. The density profile of the ctr-ECCD plasma is hollower than those of the bal-ECCD and the co-ECCD plasmas, indicating that the particle transport of these plasmas is different. The T_i profile of the ctr-ECCD plasma is similar to that of the bal-ECCD and the co-ECCD plasma as shown in figure 2(*c*), which is obtained with charge exchange spectroscopy (CXS) [22]. The heat flux is mainly due to the equipartition heating. Then, the ratio of the ion thermal diffusion coefficient of the co-ECCD plasma to that of the ctr-ECCD plasma is approximately 1.2. This ratio is smaller than the difference of electron thermal diffusion. This result can be explained as the difference in the thermal velocity between the electron and the ion. Furthermore, as shown in figure 2(*d*), the toroidal rotation velocity (V_{tor}) of the co-, bal-, and the ctr-ECCD plasmas obtained with CXS in the core region directs to the co-direction, approximately zero, and the ctr-direction, respectively. The external torque of the tangential injected NB is canceled out. Thus, the observed toroidal rotations are caused by an intrinsic torque.

3. Enhancement of particle diffusion due to stochastization

In order to evaluate particle transport from the density modulation experiment, the amplitude A^{exp} and the phase delay ϕ^{exp} profiles of the density modulation shown in figures 3(*a*) and (*b*) have been calculated by the fast Fourier transform. Here, A^{exp} is normalized by their maximum, and ϕ^{exp} is shifted to 0 at $\rho = 1$. The value of A^{exp} of the ctr-ECCD plasma at $\rho < 0.6$ is smaller than that of the co-ECCD plasma. Although ϕ^{exp} of the ctr-ECCD plasma is approximately the same as that of the co-ECCD plasma outside of $\rho \sim 0.3$, ϕ^{exp} at $\rho < 0.3$ becomes flat in the case of the ctr-ECCD plasma.

The diffusion coefficient and the convection velocity have been evaluated for the co- and the ctr-ECCD plasmas from the modulation experiment. Here, the diffusion coefficient and the convection velocity evaluated from the modulation experiment are denoted as D_{mod} and V_{mod}. The detailed analysis method for the estimation of D_{mod} and V_{mod} is shown in reference [20].

Figures 3(*c*) and (*d*) show the profiles of D_{mod} and V_{mod}. At $\rho > 0.3$, D_{mod} of the ctr-ECCD plasma is approximately the same as that of the co-ECCD plasmas within the error bars. However, D_{mod} of the ctr-ECCD plasma is 20 times larger than that of the co-ECCD plasmas inside $\rho < 0.3$ at maximum, where ι of the ctr-ECCD plasma is less than 1/3. Thus, significantly enhanced particle diffusion exists at $\rho < 0.3$. In the stochastic magnetic field, the radial particle diffusion is affected by the diffusion coefficient of field lines and the parallel particle diffusion coefficient, which is much larger than the radial particle diffusion coefficient. Thus, this result is qualitatively consistent with the theoretical result [23]. On the other

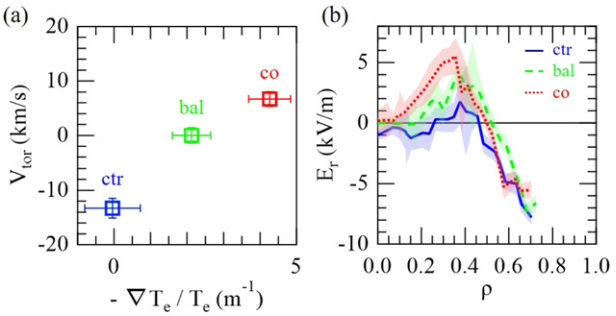

Figure 4. (*a*) Relationship between $V_{\rm tor}$ at $\rho = 0.2$ and $-\nabla T_{\rm e}/T_{\rm e}$, and (*b*) $E_{\rm r}$ profiles. The blue solid line, green dashed line, and red dotted line indicate the ctr-, bal-, and co-ECCD plasmas, respectively.

hand, $V_{\rm mod}$ of the ctr-ECCD plasma is comparable to that of the co-ECCD plasma. The core stochastization has little effect on $V_{\rm mod}$.

4. Reversal of intrinsic toroidal rotation due to stochastization

In addition to the significant change in the core diffusion, a significant difference in core momentum transport is also found. As shown in figure 2(*d*), the toroidal rotation is co-directed in the co-ECCD plasma and ctr-directed in the ctr-ECCD plasma. Since the external torque is negligible, the observed toroidal rotation is driven by the intrinsic torque.

Figure 4(*a*) shows the relationship between the core $V_{\rm tor}$ and the normalized electron temperature gradient $(-\nabla T_{\rm e}/T_{\rm e})$ in the ctr-, bal-, and co-ECCD plasmas. As the direction of the ECCD changes from the ctr-direction to the co-direction, $-\nabla T_{\rm e}/T_{\rm e}$ increases and $V_{\rm tor}$ changes from the ctr-direction to the co-direction. Figure 4(*b*) shows the change of radial electric field ($E_{\rm r}$) obtained with CXS. $E_{\rm r}$ shear at $\rho \sim 0.3$, where the toroidal rotation is different between the co- and the ctr-ECCD plasmas, is almost zero in the ctr-ECCD plasma, and increases in the bal-ECCD and further in the co-ECCD plasmas. In the ctr-ECCD case, the core magnetic field is stochastized, but in the bal-ECCD case, it is nested. Thus, the magnetic topology between the ctr- and the bal-ECCD cases is different. On the other hand, because the core magnetic field is nested both in the bal- and the co-ECCD cases, the difference in $V_{\rm tor}$ stems from the difference in the profiles between the bal- and the co-ECCD plasmas.

The difference in intrinsic rotation between the bal- and the co-ECCD cases can be argued referring to the observation in tokamak [24]. The magnetic topology is the nested magnetic flux surface in both cases. The normalized $T_{\rm e}$ gradient of the co-ECCD plasma is larger than that of the bal-ECCD plasma in the core region. On the other hand, the difference in the normalized $n_{\rm e}$ gradient and $T_{\rm i}$ gradient between the co- and the bal-ECCD plasma is small. Thus, from the difference of these profiles, the electron temperature gradient-driven trapped electron mode (TEM) is enhanced in the co-ECCD plasma [25]. This is similar to the result in tokamak: the intrinsic rotation directs to the co-current direction which is the co-direction with the toroidal magnetic field when the TEM is enhanced [24]. Because $E \times B$ shear enhances the residual stress, the higher $E_{\rm r}$ shear of the co-ECCD plasma can enhance the intrinsic torque further.

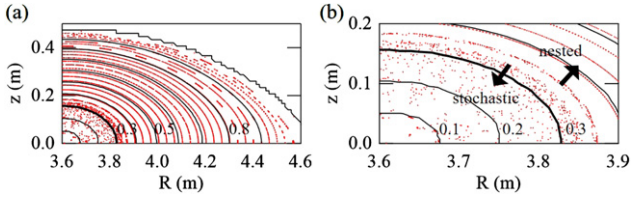

Figure 5. (*a*) Poincaré plot of the magnetic field lines for the ctr-ECCD plasma and (*b*) that focused on core region. Black lines indicate the magnetic flux surface, and thick black line indicates the magnetic flux surface at $\rho = 0.3$.

On the other hand, in the case of the ctr-ECCD plasma, since the gradients of $n_{\rm e}$, $T_{\rm e}$, and $T_{\rm i}$ are almost zero, any turbulence will not be destabilized. In addition, almost zero $E_{\rm r}$ shear will not enhance the residual stress. Therefore, the role of the intrinsic rotation due to turbulence is probably negligible. It is necessary to find new physics mechanisms to account for the ctr-directed intrinsic rotation in the stochastic magnetic field.

5. Process of stochastization

Finally, we discuss the generation process of the stochastic magnetic field. Figures 5(*a*) and (*b*) show the Poincaré plot of magnetic field lines under the experimental condition for the ctr-ECCD plasmas. Here, the magnetic field lines have been calculated by a 3D equilibrium code (HINT [26]) and a magnetic field tracing code (MGTRC [27]). In the 3D equilibrium calculation, the pressure profile is given consistent profiles of $n_{\rm e}$ and $T_{\rm e}$ with Thomson scattering measurement. Here, the current profile is determined so that ι becomes 1/3 at $\rho \sim 0.1$–0.15 which is the center of the flat region of $n_{\rm e}$ and $T_{\rm e}$ because the O-point of the magnetic island is considered to be in the center of the flat region and ambiguity of the MSE measurement is considered to exist in the core region. As shown in figure 5, the stochastization occurs at $\rho \sim 0.3$. The process of stochastization is explained as follows. The magnetic island occurs at $\iota = 1/3$ due to the ctr-ECCD current. Then, the stochastic layer is produced around the separatrix of the magnetic island [28]. Because of the low magnetic shear around $\iota = 1/3$, the disturbance of the only separatrix of $m/n = 3/1$ island grows up by error field (m: poloidal mode number, n: toroidal mode number). The magnetic flux surface at $\rho < 1/3$ becomes stochastic as shown by the red dots in figure 5.

In the bal- and the co-ECCD cases, the stochastic magnetic field does not exist at $\iota \sim 1/3$ and $\iota \sim 1/2$, respectively, because these plasmas have peaked $T_{\rm e}$ profiles. Whether the stochastization occurs or not is determined by the combination of the amplitude of the magnetic perturbations, the mode number, and the magnetic shear. For example, in reference [8], the stochastization occurs at $\iota \sim 1/2$ and the magnetic shear $\sim$0.5. However, in the co-ECCD case, the magnetic shear is approximately 0.3. On the other hand, in the bal-ECCD case, the magnetic shear is approximately 0.1, which is lower than the 0.25 of the ctr-ECCD case. These differences are

probably one of the reasons why the magnetic field of the co- and the bal-ECCD plasmas is not stochastized. The investigation of the condition of stochastization at the rational surface is a future task.

6. Summary

This paper has described the effect of the stochastic magnetic field on particle and momentum transport by comparing the co- and the ctr-ECCD plasmas. This result avails of not only the comprehension of the physics in transport in the stochastic magnetic field but also the control of transport in the plasma core.

In the core region of the ctr-ECCD plasma, the electron temperature profile has become flat inside the position of $\iota = 1/3$. This result shows the existence of large electron thermal transport and the stochastic magnetic field inside the rational surface with $\iota = 1/3$. From the density modulation experiment, D_{mod} in the stochastic magnetic field was approximately 20 times larger than that in the nested magnetic flux surface. The enhancement of particle transport in the stochastic magnetic field has been revealed experimentally by the density modulation method, which was not identified in the previous NBCD experiment [8]. In addition, V_{mod} in the stochastic magnetic field of the ctr-ECCD plasma is comparable to that of the co-ECCD plasma. Ctr-directed intrinsic toroidal rotation has been observed in the ctr-ECCD plasma. In reference [8], when flow damping occurred in the stochastic magnetic field, the toroidal flow did not become completely zero, but a ctr-directed toroidal flow remained. Because the external torque existed due to the ctr-NBI, the remains of the ctr-directed flow stemmed from the non-diffusive term and/or the remains of the external counter torque. In this paper, the ctr-directed flow that stems from the non-diffusive term has been revealed. This phenomenon is probably not explained by the intrinsic torque due to the $E \times B$ shear and the turbulence because of the small E_{r} and the small gradients of n_{e}, T_{e}, and T_{i}.

The stochastic magnetic field was reproduced by using the HINT and the MGTRC code under the experimental conditions. As a result, the magnetic flux surface of the ctr-ECCD plasma which reached $\iota \sim 1/3$ in the core region became stochastic because the disturbed magnetic flux surface at the separatrix of the magnetic island was enhanced due to the low magnetic shear.

Acknowledgments

This work is performed with the support and under the NIFS Collaboration Research program (NIFS17ULHH013, NIFS18ULHH013, NIFS18KLER045, NIFS18KLPH032, NIFS18KUHL083, NIFS19KLPH038). This work is supported by JSPS (the Japan Society for the Promotion of Science) Grant-in-aid for Scientific Research (B) 16H04620, and the NINS (National Institute of Natural Sciences) program of Promoting Research by Networking among Institutions (Grant Number KEIN1605). Also, this work was partially supported by 'PLADyS', JSPS Core-to-Core Program, A. Advanced Research Networks.

ORCID iDs

Yoshiaki Ohtani https://orcid.org/0000-0003-3646-5427
Kenji Tanaka https://orcid.org/0000-0002-1606-3204
Katsumi Ida https://orcid.org/0000-0002-0585-4561
Yasuhiro Suzuki https://orcid.org/0000-0001-7618-6305
Yuki Takemura https://orcid.org/0000-0003-3754-897X
Takahiro Bando https://orcid.org/0000-0003-1493-9185

References

[1] De Bock M.F.M., Classen I.G.J., Busch C., Jaspers R.J.E., Koslowski H.R. and Unterberg B. 2008 The interaction between plasma rotation, stochastic fields and tearing mode excitation by external perturbation fields *Nucl. Fusion* **48** 015007
[2] Park G., Chang C.S., Joseph I. and Moyer R.A. 2010 Plasma transport in stochastic magnetic field caused by vacuum resonant magnetic perturbations at diverted tokamak edge *Phys. Plasmas* **17** 102503
[3] Evans T.E. *et al* 2004 Suppression of large edge-localized modes in high-confinement diii-d plasmas with a stochastic magnetic boundary *Phys. Rev. Lett.* **92** 235003
[4] Biewer T.M. *et al* 2003 Electron heat transport measured in a stochastic magnetic field *Phys. Rev. Lett.* **91** 045004
[5] Bartiromo R., Martin P., Martini S., Bolzonella T., Canton A., Innocente P., Marrelli L., Murari A. and Pasqualotto R. 1999 Core transport improvement during poloidal current drive in the RFX reversed field pinch *Phys. Rev. Lett.* **82** 1462
[6] Inagaki S. *et al* 2004 Observation of reduced heat transport inside the magnetic island o point in the large helical device *Phys. Rev. Lett.* **92** 055002
[7] Ida K. *et al* 2013 Topology bifurcation of a magnetic flux surface in magnetized plasmas *New J. Phys.* **15** 013061
[8] Ida K. *et al* 2015 Flow damping due to stochastization of the magnetic field *Nat. Commun.* **6** 5816
[9] Ida K. *et al* 2014 Topology bifurcation of a magnetic flux surface in toroidal plasmas *Plasma Phys. Control. Fusion* **57** 014036
[10] Yoshimura Y. *et al* 2016 Improvement in flexibility of ECCD by upgraded ECH antenna system on LHD *Plasma Fusion Res.* **11** 2402036
[11] Yoshimura Y. *et al* 2012 Eccd experiment using an upgraded ech system on lhd *Plasma Fusion Res.* **7** 2402020
[12] Yamada H. *et al* 2005 Characterization of energy confinement in net-current free plasmas using the extended international stellarator database *Nucl. Fusion* **45** 1684
[13] Igami H. *et al* 2019 Recent ECRH/ECCD experiments aiming for higher density and temperature operations in the LHD *EPJ Web Conf.* **203** 02001
[14] Ida K., Yoshinuma M., Suzuki C., Kobuchi T. and Watanabe K.Y. 2010 Measurements of rotational transform with motional Stark effect spectroscopy *Fusion Sci. Technol.* **58** 383
[15] Nagaoka K. *et al* 2013 3-D effects on viscosity and generation of toroidal and poloidal flows in LHD *Phys. Plasmas* **20** 056116
[16] Takahashi H. *et al* 2018 Realization of high T_{i} plasmas and confinement characteristics of ITB plasmas in the LHD deuterium experiments *Nucl. Fusion* **58** 106028
[17] Suzuki C., Ida K., Suzuki Y., Yoshida M., Emoto M. and Yokoyama M. 2012 Development and application of real-time magnetic coordinate mapping system in the large helical device *Plasma Phys. Control. Fusion* **55** 014016

[18] Tanaka K. *et al* 2006 Analysis scheme for density modulation experiments to study particle confinements *Plasma Sci. Technol.* **8** 65
[19] Tanaka K. *et al* 2008 Density reconstruction using a multichannel far-infrared laser interferometer and particle transport study of a pellet-injected plasma on the LHD *Plasma Fusion Res.* **3** 050
[20] Ohtani Y., Tanaka K., Tokuzawa T., Akiyama T., Yamada L., Yasuhara R., Funaba H., Shoji M. and Goto M. 2020 Particle transport of electron cyclotron resonant heating plasma in large helical device *Plasma Phys. Control. Fusion* **62** 025029
[21] Shi N. *et al* 2014 Electron density reconstruction and optimum beam arrangement of far-infrared interferometer in heliotron J *Plasma Fusion Res.* **9** 3402043
[22] Yoshinuma M., Ida K., Yokoyama M., Osakabe M. and Nagaoka K. 2010 Charge-exchange spectroscopy with pitch-controlled double-slit fiber bundle on LHD *Fusion Sci. Technol.* **58** 375
[23] Laval G. 1993 Particle diffusion in stochastic magnetic fields *Phys. Fluids* B **5** 711
[24] Rice J.E. *et al* 2011 Rotation reversal bifurcation and energy confinement saturation in tokamak Ohmic *L*-mode plasmas *Phys. Rev. Lett.* **107** 265001
[25] Nakata M., Nagaoka K., Tanaka K., Takahashi H., Nunami M., Satake S., Yokoyama M. and Warmer F. 2019 *Plasma Phys. Control. Fusion* **61** 014016
[26] Suzuki Y., Nakajima N., Watanabe K., Nakamura Y. and Hayashi T. 2006 Development and application of HINT2 to helical system plasmas *Nucl. Fusion* **46** L19–24
[27] Itagaki M., Okubo G., Akazawa M., Matsumoto Y., Watanabe K., Seki R. and Suzuki Y. 2012 Use of a twisted 3D cauchy condition surface to reconstruct the last closed magnetic surface in a non-axisymmetric fusion plasma *Plasma Phys. Control. Fusion* **54** 125003
[28] Abdullaev S.S. 2006 *Construction of Mappings for Hamiltonian Systems and Their Applications* (Berlin: Springer)